Received: 10 January 2017 | Revised: 10 April 2017 | Accepted: 16 May 2017

DOI: 10.1002/ima.22228

RESEARCH ARTICLE

WILEY

Fusion of MRI and CT images using guided image filter and image statistics

Durga Prasad Bavirisetti[1] | **Vijayakumar Kollu**[2] | **Xiao Gang**[1] | **Ravindra Dhuli**[2]

[1] School of Aeronautics and Astronautics, Shanghai Jiao Tong University, Shanghai 200240, People's Republic of China

[2] School of Electronics Engineering, VIT University, Vellore 632014, Tamil Nadu, India

Correspondence
Gang Xiao, School of Aeronautics and Astronautics, Shanghai Jiao Tong University, Shanghai 200240, People's Republic of China.
Email: xiaogang@sjtu.edu.cn

Funding information
National Program on Key Basic Research Project, Grant/Award Number: 2014CB74 4903; National Natural Science Foundation of China, Grant/Award Number: 61673270; Shanghai Pujiang Program, Grant/Award Number: 16PJD028; Aerospace Science and Technology Innovation Foundation, Grant/Award Number: HTKJCX2015CAAA09

Abstract

In medical imaging using different modalities such as MRI and CT, complementary information of a targeted organ will be captured. All the necessary information from these two modalities has to be integrated into a single image for better diagnosis and treatment of a patient. Image fusion is a process of combining useful or complementary information from multiple images into a single image. In this article, we present a new weighted average fusion algorithm to fuse MRI and CT images of a brain based on guided image filter and the image statistics. The proposed algorithm is as follows: detail layers are extracted from each source image by using guided image filter. Weights corresponding to each source image are calculated from the detail layers with help of image statistics. Then a weighted average fusion strategy is implemented to integrate source image information into a single image. Fusion performance is assessed both qualitatively and quantitatively. Proposed method is compared with the traditional and recent image fusion methods. Results showed that our algorithm yields superior performance.

KEYWORDS

brain, guided image filter, image fusion, image statistics, medical

1 | INTRODUCTION

In medical imaging,[1,2] different modalities such as positron emission tomography (PET), single photon emission tomography (SPECT), computer tomography (CT), and magnetic resonance imaging (MRI) are used to capture complementary information. For example, as shown in Figure 1, CT image (left-hand side) provides hard tissue information such as bone structure, whereas MRI image (right-hand side) provides soft substance information such as flesh. However, a radiologist needs both CT and MRI information in a single image for better diagnosis and treatment. Hence, useful or complementary information from different sensing technologies has to be integrated into an image. Image fusion is a process of combining useful and complementary information of source images into a single image. This fused image is helpful in computer assisted surgery and radio surgery. In this article, we concentrated on fusion of CT and MRI images of "human brain."

Fusion process can be performed at three levels. They are pixel or signal level, objective or feature level and symbolic or decision level. In pixel-level image fusion, the process of fusion is performed on information present in the co-registered input imagery pixel by pixel. Contribution in this area can be found in Refs. 3–5. In objective level image fusion, property descriptors, features, and object labels derived from each source image are used for fusion.[6] Symbolic level image fusion is a high-level fusion. Here, local decision makers are derived from objective level fusion results. Finally, fusion is employed on probabilistic decision information extracted from these decision makers.[7] This article focuses on pixel-level fusion.

The remaining article is organized as follows. Section II briefs the related work. Section III presents the proposed method. Section IV describes the fusion metrics. In Section V, experimental setup is discussed. Section VI presents the results and analysis. Section VII concludes the article.

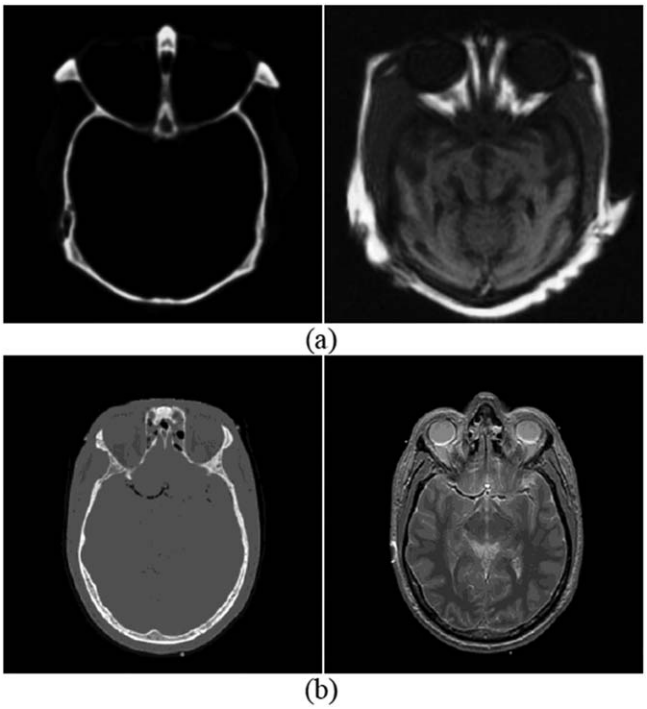

FIGURE 1 CT and MRI images: (A) dataset 1 and (B) dataset 2

2 | RELATED WORK

An efficient pixel-level image fusion[8] algorithm should satisfy the following three requirements:

1. It should preserve the necessary information from input imagery.
2. It should not produce artifacts.
3. It should not depend on location and orientation of the objects present in the source imagery.

In this context, for the past few decades, several pixel-level image fusion algorithms have been developed for spatially register images. Pixel-level image fusion can be classified in a generic way based on the methods used, namely, nonlinear operator, optimization, artificial neural network, multiresolution decomposition, and edge preserving-based methods. In nonlinear methods, min, max, and morphological nonlinear operators are used for the purpose of fusion. Successful fusion methods based on morphological operators are discussed in Refs. 9–11. Even though these methods are simple, fused image may not look good. In optimization-based approaches,[12,13] fusion process is expressed as Bayesian optimization problem. But in general, this problem is difficult to solve. Markov random field[14] and generalized random walk[15] methods solve this problem by computing edge aligned weights. Fused image may be over smoothened because of multiple iterations. Furthermore, artificial neural networks have gained a lot of interest in the area of image fusion by the inspiration of biological signal fusion. Successful methods in this class are discussed in Refs. 16–21.

In addition to the above fusion schemes, multiresolution schemes have played a great role in image fusion. These schemes are motivated by the fact that human visual system (HVS) is sensitive to the edge information. That is, HVS can perceive even small changes in edge information. Both image pyramid and wavelet decomposition belong to multiresolution methods. These approaches require transform domain analysis. Image pyramid decomposes each given image into set of low-pass filtered images. Each filtered image represents the information of the given image in different scales.[22–25] Gradient pyramid (Grad),[23] laplacian pyramid,[24] ratio of low-pass pyramid (Ratio),[22] Gaussian pyramid,[25] contrast pyramid, filter-subtract-decimate pyramid, and morphological pyramid[26] methods are used for the purpose of fusion.

Succeeding fusion schemes in this category of multiresolution category uses discrete wavelet transform (DWT) decompositions.[27–30] DWT has more advantages over pyramid. It provides compact representation and directional information of a given image. These qualities of DWT make it suitable for the purpose of fusion. Wavelet fused image contains less blocking effects than pyramid fused image. DWT is shift variant because of its multirate operations. This shift variant property may introduce some artifacts in the fused image. To avoid these problems of DWT, stationary wavelet transform (SWT) has been introduced.[31–33] SWT image fusion methods can be found in Refs. 34,35. Image fusion is also carried out using recent techniques such as singular value decomposition (SVD),[36] high order singular value decomposition,[37] and two-scale fusion (TIF).[38,39]

Final category of image fusion schemes are edge preserving techniques. Among them edge preserving L_0-gradient minimization,[40] weighted least filter,[41] guided image filters (GFF),[42] and anisotropic diffusion[43] are the recently proposed edge preserving-based image fusion methods. Edge preserving filters are more reliable to extract salient information (lines and details) compared to some of the multiscale decomposition techniques.[44] For example, pyramid decomposition[24] may produce halo effects near the edges because of linear filtering, whereas these filters use nonlinear filtering for this purpose.

We prefer guided image filter (GF) for salient information extraction from detail layers. This filter is a recently proposed edge preserving filter which provides best edge information. It offers a good tradeoff between edge preservation and blurring. Unlike anisotropic diffusion,[45] it is a non-iterative approach with less computational time. In this article, we propose a new weighted superposition image fusion method using edge-preserving guided image filter.

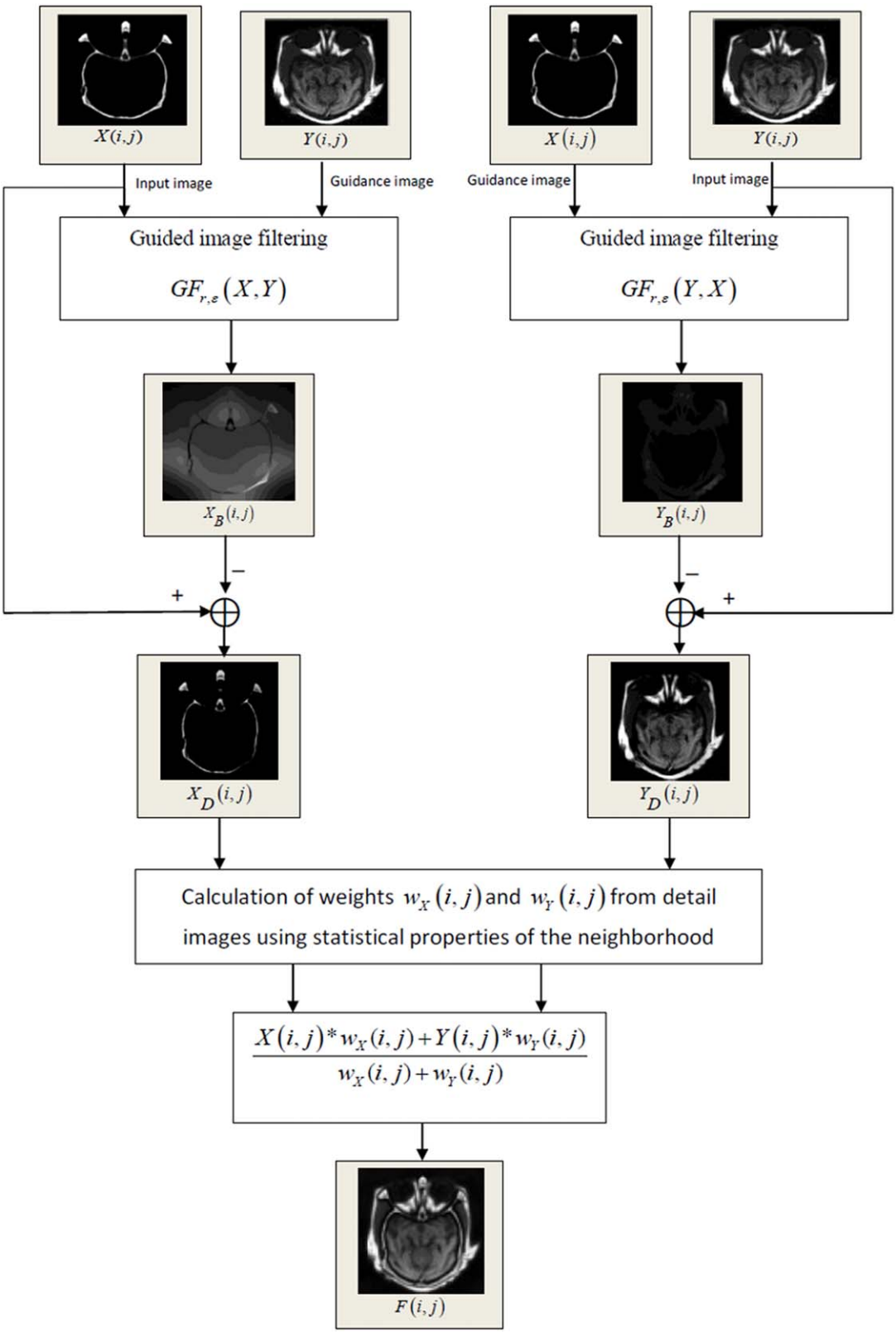

FIGURE 2 Proposed method [Color figure can be viewed at wileyonlinelibrary.com]

3 | PROPOSED METHOD

The key idea in our proposed method is blur the source images using GF, then subtract these blurred images from corresponding source images to get sharpen images. Use details of sharpened images to calculate weights for the purpose of fusion. The proposed method is illustrated in Figure 2. For better understanding, we have explained this method

with the help of images by detailing the changes in each and every step. This algorithm consists of two major steps. (A) First step: obtain the detail layer images using GF. (B) Second step: fuse the detail images using a fusion rule based on image statistics. The proposed method is explained as follows.

3.1 | Guided image filter

Guided image filter (GF)[46] is an explicit image filter. This filter computes the output of a pixel in an image by taking the statistics of the neighborhood around that pixel into the account. It is a local linear model between output and guidance image. GF computes the output like other linear transform invariant (LTI) filters[47] but it uses a second image to filter the input image for guidance purpose. Second image may be the same input image or a translated version of it or a totally a different image. This filter is an edge-preserving smoothing filter,[45,48,49] which not only smooths the input image but also preserves the edge information.

If G is a guidance image centered at a pixel l in a local square window w_l, then the filtered output O at a pixel j is given by

$$O_j = m_l G_j + n_l, \forall j \in w_l, \tag{1}$$

where m_l and n_l are the linear coefficients which are constant in window w_l. To determine linear coefficients (m_l, n_l), constraints have to be derived from the input image I.

In other way, to get noise free output, unwanted components N (like noise or texture) must be subtracted from I.

$$O_j = I_j - N_j, \tag{2}$$

The solution for this problem should minimize the difference between I and O. It should also maintain the relation in Equation 1. Hence, m_l and n_l are the linear coefficients that can minimize the cost function in window w_l as

$$E(m_l, n_l) = \sum_{j \in w_l} ((m_l G_j + n_l - I_j)^2 + \varepsilon m_l^2), \tag{3}$$

where ϵ is the regulization parameter. Equation 3 represents the linear regression model.[50,51] The solution for this is directly given by

$$m_l = \frac{\frac{1}{|w|}\sum_{j \in w_l} G_j I_j - \mu_l \overline{I_l}}{\sigma_l^2 + \varepsilon}, \tag{4}$$

$$n_l = \overline{I_l} - m_l \mu_l \tag{5}$$

Here, $|w|$ is the number of pixels in the window w_l centered at pixel l, μ_l is the mean, and σ_l^2 is the variance in the window w_l. $\overline{I_l}$ is the mean of input I_l in w_l and is given by $\overline{I_l} = \frac{1}{w}\sum_{j \in w_l} I_j$. Once linear coefficients are obtained, then output O_j can be solved according to Equation 1. But different overlapping windows w_l centered at l contain pixel j in common. To resolve this problem, take average of all estimates of O_j. Hence, the filtering output can be given as

$$O_j = \overline{m_j} G_j + \overline{n_j}, \tag{6}$$

where $\overline{m_j} = 1/|w| \sum_{l \in w_j} m_j$ and $\overline{n_j} = 1/|w| \sum_{l \in w_j} n_j$ are the averages of all linear coefficients. In this article, guided image filtering output of I in the guidance of G is denoted as $GF_{r,\varepsilon}(I, G)$, where r is the filter size/neighborhood size and ε is the degree of smoothing/regulization parameter. The behavior of the GF controlled by these parameters r and ε. If the guidance image has a variance $\sigma^2{}_l$ higher than the threshold, $\varepsilon(\sigma^2{}_l \geq \varepsilon)$ within a window w_l, then the pixel in the center of the window remain unchanged, whereas if a pixel is in the center of low variance window whose variance is less than $\varepsilon(\sigma^2{}_l \leq \varepsilon)$, then pixel value is replaced by the average of the neighborhood.

Some major applications of GF include edge preserving smoothing, image matting, feathering HDR compression, and detail enhancement. Along with edge-preserving filtering, two properties—structure transferring and gradient preserving—make GF qualify for the purpose of image fusion.

3.1.1 | Structure transferring filtering

This is one of the important properties of GF. If the guidance image is same as the input image then there is no impact on the structure of input image. However, the guided image is different from the input image then structures of the guidance image influence the input image.

3.1.2 | Gradient preserving filtering

Besides edge-preserving filtering like bilateral filter,[49] joint bilateral filters[48] GF can also avoid gradient reversal artifacts during filtering process. Because of these qualities this filter is also used in detail enhancement.[52] In detail enhancement, edge aware smoothing filtered output treated as base layer B for the input I. Detail layer D is computed as $D_i = I_i - B_i$. Manipulated detailed layer is combined with base layer to get enhanced image. Compared to bilateral filter, guided filter performs better near edges because of gradient preserving.[46]

3.2 | Image fusion rule

A new fusion scheme is proposed in Ref. 53 and adopted in Ref. 54. The fusion scheme uses weighted average scheme for the purpose of fusion. Using statistical properties, this method finds optimal weights adaptively. The fusion rule is discussed as follows.

The basic idea is to find weight corresponding to a pixel in an image based on its horizontal and vertical edge

strengths. In theory, to find a weight corresponding to a pixel at a location (*x, y*) in an image take a square window *w* of size $m \times m$ around its neighborhood. Consider Z as a matrix and find its covariance matrix ($\mathrm{cov}(Z)$) by considering row as an observation, column as a variable.

$$\mathrm{cov}(Z) = E\left[(Z - E[Z])(Z - E[Z])^T\right] \tag{7}$$

Calculate unbiased estimate ${C_H}^{x,y}(Z)$ of a covariance matrix at a pixel location (x, y) as

$$C_H^{x,y}(Z) = \frac{1}{m-1}\sum_{j=1}^{m}\left(Z_j - \overline{Z}\right)\left(Z_j - \overline{Z}\right)^T \tag{8}$$

where Z_j is the *j-th* observation of the *m*-dimensional variable and $\overline{Z}$ is the average of the observation. Interestingly diagonal of ${C_H}^{x,y}(Z)$ is a variance vector. Compute Eigen values λ_H^j of ${C_H}^{x,y}(Z)$. As the size of matrix is $m \times m$, number of Eigen values can be find is *m*. To get horizontal edge strength α_H. Add all these Eigen values.

$$\alpha_H(x, y) = \sum_{j=1}^{m}\lambda_H^j. \tag{9}$$

Similarly, to take vertical edge strength into account, take every column as an observation and row as a variable. Calculate the unbiased estimate $C_V^{x,y}$, and then compute the Eigen values λ_V^j of $C_V^{x,y}$. Add these Eigen values to get the vertical edge strength α_V as,

$$\alpha_V(x, y) = \sum_{j=1}^{m}\lambda_v^j \tag{10}$$

To find the weight $W(x, y)$ of a pixel at location(x, y), take the sum of $\alpha_H(x, y)$ and $\alpha_V(x, y)$.

$$W(x, y) = \alpha_H(x, y) + \alpha_V(x, y) \tag{11}$$

Repeat this process for each and every pixel present in the image to assign weights adaptively. Here, weight of a pixel depends on its edge strength but not on its intensity value.

As shown in Figure 2, source images $X(i,j)$ and $Y(i,j)$ are applied to the GF. Here, left-hand side (LHS) and right-hand side (RHS) indicate the same process till getting detail layer images from source images. In LHS process, source images $X(i,j)$ and $Y(i,j)$ act as input image and guidance image, respectively, for GF. This filter performs edge preserving smoothing operation on input image $X(i,j)$ in the guidance of the image $Y(i,j)$. If two source images are different, then this filter performs structure transferring property to smooth the input. The GF operation is given as $GF_{r,\varepsilon}(X, Y)$. Output of $GF_{r,\varepsilon}(X, Y)$ gives a base layer $X_B(i,j)$. Finally, detail layer $X_D(i,j)$ is obtained by subtracting the base layer $X_B(i,j)$ from an input image $X(i,j)$. In RHS process, source images $X(i,j)$ and $Y(i,j)$ act as guidance image and input image, respectively, unlike in LHS process. Except this, everything is the same as in the LHS process.

In the second step, using the image statistics, weights $W_X(i,j)$ and $W_Y(i,j)$ are calculated from detail images. After finding weights for the corresponding source images, a simple weighted average method is used to obtain fused image $F(i,j)$.

4 | FUSION EVALUATION METRICS

The purpose of image fusion is to preserve all useful information in the source images. During this process, it should not produce any artifacts. To verify the effectiveness of a given fusion algorithm, we need some quantitative measures. Many fusion metrics[5,55–58] have been proposed in the literature. Latest among them is *Petrovic Metric*.[55] A brief discussion of performance evaluation is presented below. Consider an input image $f(m, n)$ of size $p \times q$.

4.1 | Mean ($\overline{F}$) or average pixel intensity (μ)

Measures the contrast of the fused image,

$$\overline{F} = \mu = \frac{\sum_{m=1}^{p}\sum_{n=1}^{q} f(m, n)}{pq}, \tag{12}$$

where $f(m, n)$ is the intensity value at the pixel location (m, n).

4.2 | Standard deviation (SD or σ)

It indicates spread in the data, that is, the variation of the current pixel intensity value with respect to the average pixel intensity value in the fused image.

$$SD = \sigma = \sqrt{\frac{\sum_{m=1}^{p}\sum_{n=1}^{q}\left(f(m, n) - \overline{F}\right)^2}{pq}}, \tag{13}$$

4.3 | Average gradient (AG)

The degree of clarity and sharpness in the fused image is given by average gradient as

$$\mathrm{AG} = \sum_{m=1}^{p}\sum_{n=1}^{q}\frac{\sqrt{((f(m, n) - f(m+1, n))^2 + ((f(m, n) - f(m, n+1))^2)}}{pq} \tag{14}$$

4.4 | Mutual information (MI) or fusion factor

It measures the overall information present in the fused image with respect to the source images and is given by

$$MI = MI_{XF} + MI_{YF}, \tag{15}$$

where $MI_{XF} = \sum_m \sum_n p_{X,F}(m,n) \log_2 \left(\frac{p_{X,F}(m,n)}{p_X(m) p_F(n)} \right)$ is the mutual information between source image X and fused image F. Here $p_X(m)$ and $p_F(n)$ indicate the probability density functions of source images X and Y, respectively. $p_{X,F}(m,n)$ is the joint probability density function of source image X and the fused image F. Similarly MI_{YF} is the mutual information between Y and F.

Similarly, r_{YF} represents the correlation coefficient between source image Y and fused image F.

4.5 | Spatial frequency (SF)

This metric is used to find overall information level (activity level) present in the regions of the fused image and is given by the square root of summation of squares of row frequencies (RF) and column frequencies (CF).

$$SF = \left(RF^2 + CF^2 \right)^{\frac{1}{2}}, \tag{16}$$

where $RF = \sqrt{\frac{\sum_m \sum_n (f(m,n) - f(m,n-1))^2}{pq}}$,

$$CF = \sqrt{\frac{\sum_m \sum_n (f(m,n) - f(m-1,n))^2}{pq}}.$$

Based on the gradient information representation, an objective image fusion performance characterization[55] is considered in addition to above fusion performance evaluation metrics. This method provides much deeper insight into the benefits and drawbacks of image fusion methods by estimating information contribution of every source image by measuring the fusion gain.

4.6 | Fusion information score $Q^{XY/F}$

If X and Y are the two source images and F is a fused image, then fusion information score is represented as $Q^{XY/F}$. It is a gradient-based fusion performance metric. This metric assesses the fusion algorithm performance based on the amount of edge information transfer from the source image to the fused image. For complete details, one may refer to Refs. 55,58. This metric satisfies $0 \leq Q^{XY/F} \leq 1$. If $Q^{XY/F} = 0$, then it implies the complete loss of source information. If $Q^{XY/F} = 1$, then it indicates the "ideal fusion" with no loss of source information.

Using all the metrics presented so far, the performance of our proposed algorithm is compared with the recent image fusion algorithms.

5 | EXPERIMENTAL SETUP

Here we discuss about the image database, various fusion algorithms used for comparison, and the effect of free parameters on our proposed algorithm. For better understanding, experiments and analysis of the proposed algorithm are presented for two datasets. However, proposed fusion algorithm can also yield good results for random image datasets of our choice.

5.1 | Image database

Experiments are performed on medical image datasets presented in Figure 1. They referred to as dataset 1 and dataset 2, respectively. These datasets are collected from http://www.med.harvard.edu/AANLIB/home.html.

5.2 | Other image fusion methods for comparison

Proposed image fusion algorithm is compared with other image fusion algorithms depends on pyramid based methods (Grad,[23] Ratio[22]), Wavelet based method SWT,[35] SVD,[36] and GFF[42] (these methods are referred with the techniques/transforms that are used for the purpose of image fusion). The default parameter settings suggested by the concerned authors have been adopted for all these methods.

5.3 | Analysis of fusion metrics

Along with traditional image fusion metrics μ, σ, *AG*, *MI*, *SF*, objective fusion metric $Q^{XY/F}$ is also considered to verify the effectiveness of the proposed algorithm. The objective of any fusion algorithm is to generate a qualitative fused image. For better quality, fused image should have high values for all these metrics. The fusion metric with highest value is highlighted in bold letter.

5.4 | Analysis of free parameters

Here the effect of free parameters on the fusion algorithm is discussed. In the proposed method, first each source image is low-pass filtered using the GF. Next, weights are calculated by considering image statistics of the filtered image. The amount of low-pass filtering depends on the degree of blur ϵ and the filter size r. The effect of free parameters r, ε on the proposed algorithm is carried out with help of average metric values calculated over medical image data sets. When analyzing the effect of ε on the proposed algorithm, remaining parameters

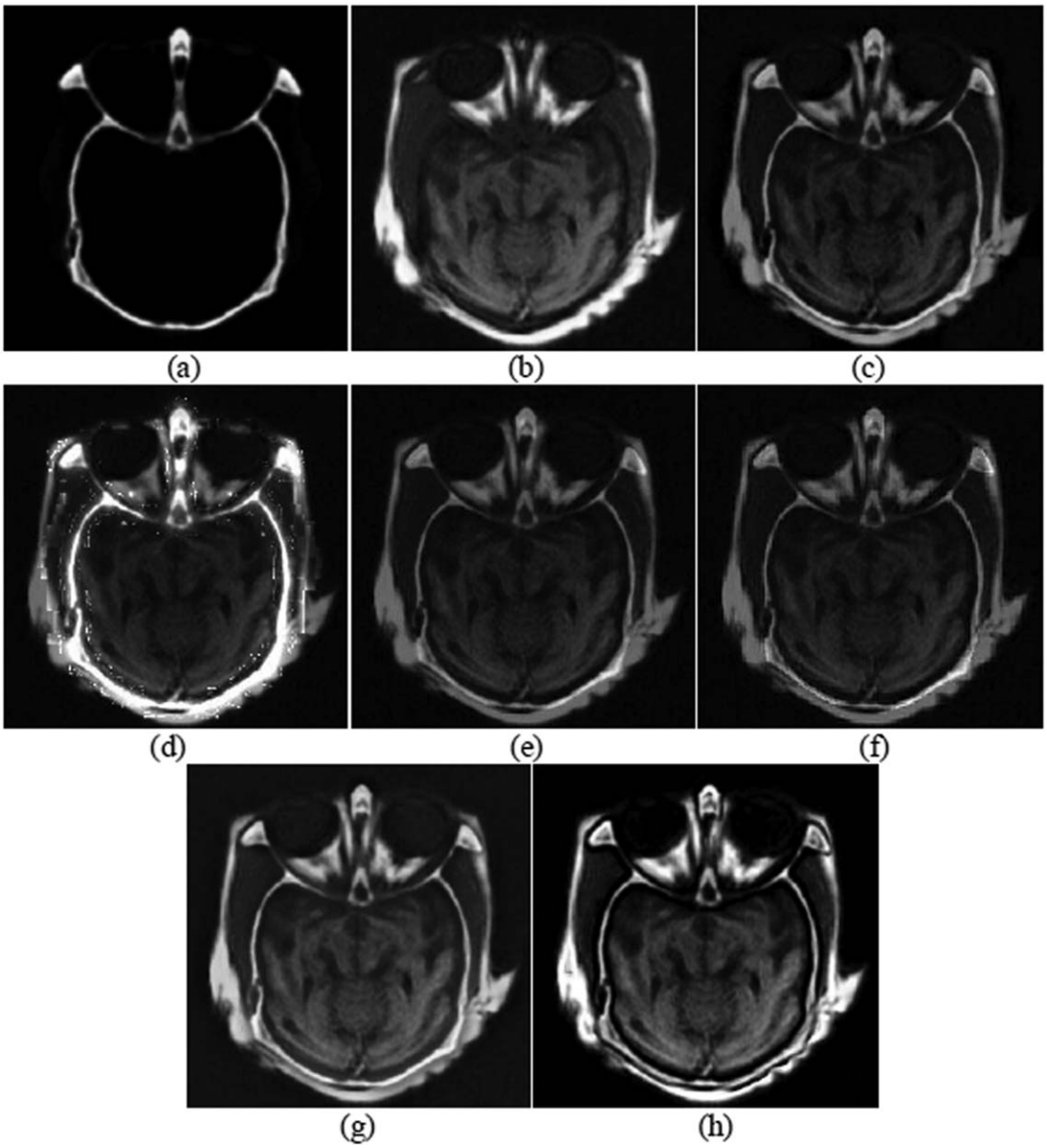

FIGURE 3 Visual quality analysis of various fusion methods on dataset 1: (A) CT image, (B) MRI image, (C) Grad, (D) ratio, (E) SWT, (F) SVD, (G) GFF, and (H) proposed method

values are considered as $r=25$ and $w=5$. Similarly, while inspecting the effect of r, $\varepsilon=2.1$ and $w=5$ are considered. To know the effect of ε on the proposed method, vary the ε from minimum to maximum value and note down the average fusion metric values to observe the performance. One can note that the performance of the proposed algorithm is almost constant for change of ε. Similarly, the effect of r on our method is also analyzed. It is observed that the performance of fusion metrics are almost constant after $r=5$. Hence, the default parameter settings considered for simulations are $r=25$ and $\varepsilon=2.1$. While calculating the weights for the fusion rule, experimented with different window sizes $w=3,5,7,9$. It is observed that if w increases some fusion metrics perform better while other metrics failed to give good performance. For $w = 5$, we observed appreciable performance in all fusion metrics.

6 | RESULTS AND ANALYSIS

Aim of any fusion algorithm is to integrate required information from both source images in the output image. Fused image cannot be judged exclusively by seeing the fused image or by measuring fusion metrics. It should be judged qualitatively using visual display and quantitatively using fusion metrics. In this section, we are presenting both visual quality and quantitative analysis of various algorithms.

6.1 | Qualitative analysis

Consider brain images captured using CT and MRI modalities as shown Figure 1. As we discussed in Section 1, CT can capture boney structure or hard tissues, whereas MRI

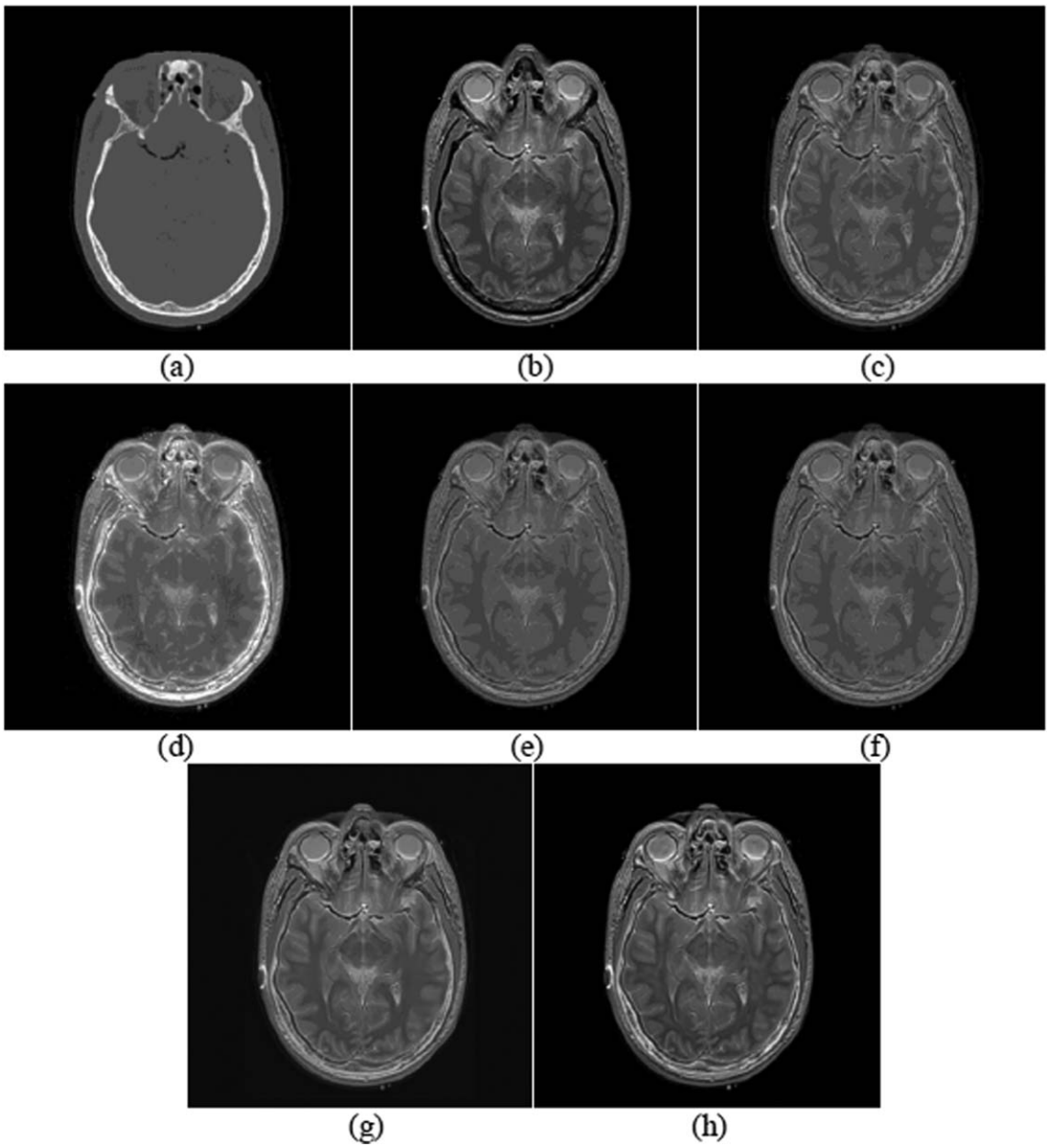

FIGURE 4 Visual quality analysis of various fusion methods on dataset 2: (A) CT image, (B) MRI image, (C) Grad, (D) ratio, (E) SWT, (F) SVD, (G) GFF, and (H) proposed method

can capture soft tissues present in the brain. However, for better diagnosis and treatment of a disease, it is necessary to integrate all the required information of these images into one image using fusion process.

Visual quality analysis of various fusion methods for image dataset 1 is presented in Figure 3. Here, Figure 3A,B shows the CT and MRI images. Fused images of Grad, Ratio, SWT, SVD, and GFF methods are displayed in Figure 3C–G, respectively. Fused image of the proposed method is displayed in Figure 3I. From the results, it can be observed that visual quality or contrast of the resultant images of Grad (Figure 3C), SWT (Figure 3E), and SVD (Figure 3F) fusion methods are not up to the mark. Ratio method is introducing some visual distortions into the fused image. Fused image (Figure 3G) of GFF method is visually looking good. However, proposed method is generating visually qualitative and undistorted image (Figure 3H) compared to that of the GFF method.

Visual quality comparison of numerous fusion algorithms for image dataset 2 is showcased in Figure 4. Source CT and MRI images are displayed in Figure 4A,B. Fused images of other methods Grad, Ratio, SWT, SVD, and GFF used for comparison are presented in Figure 4C–G, respectively. Fused image of the proposed algorithm is displayed in Figure 4H. CT image (Figure 4A) is providing hard-tissue information. MRI image (Figure 4A) is providing soft-tissue information. As shown in Figure 4C,E,F, Grad, SWT, and SVD methods are not able to integrate all the complementary information of these source images. We can observe some information loss when compared to source images. Ratio

TABLE 1 Quantitative analysis of different image fusion algorithms for CT and MRI dataset 1

	Method					
Metric	**Grad**	**Ratio**	**SWT**	**SVD**	**GFF**	**Proposed**
μ	34.4567	41.4675	32.0840	32.0722	50.7287	**53.5475**
σ	41.2549	48.5089	35.1070	35.9378	55.4783	**58.8670**
AG	7.6165	7.2423	6.2333	7.4496	9.5527	**11.7035**
MI	2.9574	3.2294	4.1030	3.4463	3.3884	**4.1796**
SF	14.0942	15.9918	11.3612	15.0588	17.4649	**21.0772**
$Q^{XY/F}$	0.8603	0.6965	0.6760	0.7544	0.9073	**0.9120**

method is degrading the fused image quality. GFF method is able integrate all the required information and able to generate visually good image. However, proposed method's fused image is providing visually more details compared to GFF method. Our fused image contrast is also good compared to that of the state-of-the-art methods.

6.2 | Quantitative analysis

The quantitative analysis of the proposed method in comparison with various fusion methods is done with the help of fusion metrics μ, σ, AG, MI, SF, and $Q^{XY/F}$. As discussed in Section 3.1, metrics μ and σ measure the contrast. AG measures the clarity and sharpness. The overall mutual information of fused image with respect to the source images can be measured by MI. The overall activity level present the fused image can be assessed by SF. Finally, $Q^{XY/F}$ measures the total amount of edge information transferred from source images to fused image. For better performance, any algorithm should possess high metric values.

Performance evaluation of different image fusion algorithms along with the proposed algorithm for image dataset 1 is presented in Table 1. It is observed that SVD method has lowest value for metric μ. SWT has lowest σ value. AG metric value is low for SWT. Grad has lowest MI value. SF and $Q^{XY/F}$ metrics are low for SWT method. In all the metrics, GFF and proposed method are showing consistent performance. However, proposed method has maximum performance in all fusion metrics.

Performance evaluation of image dataset 2 for various methods is presented in Table 2. It can be noted that SWT has lowest performance for the fusion metrics σ, AG, SF and $Q^{XY/F}$. μ is less for Ratio method. Grad has lowest MI value. However, proposed method is showing consistency, stable, and maximum performance for all the fusion metrics as bolded in Table 2.

From the above results and analysis, it is clear that proposed method is outperforming state-of-the-art fusion methods in terms of visual quality and fusion metrics.

7 | CONCLUSION

A new pixel-level fusion algorithm is proposed to fuse CT and MRI images. First, each source image is filtered using edge aware smoothing guided filter. Weights are calculated based on statistics of the detail layers. Then fused image is obtained by taking the weighted average of the source images. Fusion performance is assessed in terms of visual quality and evaluation metrics. Results reveal that proposed

TABLE 2 Quantitative analysis of different image fusion algorithms for CT and MRI dataset 2

	Method					
Metric	**Grad**	**Ratio**	**SWT**	**SVD**	**GFF**	**Proposed**
μ	44.5866	42.7681	43.3506	43.3482	44.4982	**44.7091**
σ	52.7125	53.8372	51.7784	51.9388	55.0674	**55.2248**
AG	5.4983	6.3328	4.9077	5.4241	6.2094	**6.7729**
MI	3.5388	3.5577	3.8130	3.6153	4.0612	**4.2208**
SF	11.1936	13.3563	9.8522	11.0744	12.8377	**14.0555**
$Q^{XY/F}$	0.6942	0.6812	0.6375	0.6993	0.6964	**0.7158**

method is well suited for medical imaging. Our method showed promising results compared to the traditional and recent fusion techniques.

- Even though experiments are demonstrated for CT and MRI modalities, proposed algorithm can also be applied on other medical imaging modalities as well.
- In this article, for effective demonstration, results and analysis of two image datasets are presented. However, our fusion method can also yield better performance for a random image fusion dataset of our choice.
- Along with medical imaging, proposed method can also give reasonable performance for both single- and multisensor image fusion applications.

ACKNOWLEDGMENT

This research is sponsored by National Program on Key Basic Research Project (2014CB744903), National Natural Science Foundation of China (61673270), Shanghai Pujiang Program (16PJD028), Aerospace Science and Technology Innovation Foundation (HTKJCX2015CAAA09).

REFERENCES

[1] Liu S, Zhao J, Shi M. Medical image fusion based on improved sum-modified-Laplacian. *Int J Imag Syst Technol.* 2015;25:206–212.no.

[2] Liu S, Zhang T, Li H, Zhao J, Li H. Medical image fusion based on nuclear norm minimization. *Int J Imag Syst Technol.* 2015;25:310–316.no.

[3] Hamza A, He Y, Krim H, Willsky A. A multiscale approach to pixel-level image fusion. *Integr Comput Aid Eng.* 2005;12:135–146. no.

[4] Li H, Manjunath BS, Mitra SK. Multisensor image fusion using the wavelet transform. *Graph Models Image Process.* 1995;57:235–245.no.

[5] Petrovic V. Multisensor pixel-level image fusion PhD thesis. In: *Department of Imaging Science and Biomedical Engineering Manchester School of Engineering, United Kingdom*, 2001.

[6] Sasikala M, Kumaravel N. A comparative analysis of feature based image fusion methods. *Information Technol J.* 2007;6:1224–1230. no.

[7] Tao Q, Veldhuis R. Threshold-optimized decision-level fusion and its application to biometrics. *Pattern Recognit.* 2009;42:823–836.no.

[8] Aslantas V, Toprak AN. A pixel based multi-focus image fusion method. *Opt Commun.* 2014;332:350–358.

[9] De I, Chanda B, Chattopadhyay B. Enhancing effective depth-of-field by image fusion using mathematical morphology. *Image Vis Comput.* 2006;24:1278–1287.no.

[10] Ramac LC, Uner MK, Varshney PK, Alford MG, Ferris DD Jr. Morphological filters and wavelet-based image fusion for concealed weapons detection. In: *Aerospace/Defense Sensing and Controls*, pp. 110–119. International Society for Optics and Photonics, 1998.

[11] Yang B, Li S. Multi-focus image fusion based on spatial frequency and morphological operators. *Chinese Opt Lett.* 2007;5:452–453. no.

[12] Fasbender D, Radoux J, Bogaert P. Bayesian data fusion for adaptable image pansharpening. *IEEE Trans Geosci Remote Sens.* 2008;46:1847–1857.no.

[13] Mascarenhas NDA, Banon GJF, Candeias ALB. Multispectral image data fusion under a Bayesian approach. *Int J Remote Sens.* 1996;17:1457–1471.no.

[14] Shen R, Cheng I, Shi J, Basu A. Generalized random walks for fusion of multi-exposure images. *IEEE Trans Image Process.* 2011;20:3634–3646. no.

[15] Xu M, Chen H, Varshney PK. An image fusion approach based on Markov random fields. *IEEE Trans Geosci Remote Sens.* 2011;49:5116–5127. no.

[16] Newman EA, Hartline PH. Integration of visual and infrared information in bimodal neurons of the rattlesnake optic tectum. *Science (New York, NY).* 1981;213:789.

[17] Newman EA, Hartline PH. The infrared "vision" of snakes. *Sci Am.* 1982.

[18] Schiller PH. The color-opponent and broad-band channels of the primate visual system. In: *From Pigments to Perception*. US: Springer; 1991: 127–132.

[19] Schiller PH. The ON and OFF channels of the visual system. *Trends Neurosci.* 1992;15:86–92.no.

[20] Waxman AM, Seibert MC, Gove A, et al. Neural processing of targets in visible, multispectral IR and SAR imagery. *Neural Networks.* 1995;8:1029–1051.no.

[21] Waxman AM, Aguilar M, Fay DA, Ireland DB, Racamato JP. Solid-state color night vision: Fusion of low-light visible and thermal infrared imagery. *Lincoln Lab J.* 1998;11:41–60. no.

[22] Burt PJ. The pyramid as a structure for efficient computation. In: *Multiresolution Image Processing and Analysis*. Berlin, Heidelberg: Springer; 1984: 6–35.

[23] Burt PJ. A gradient pyramid basis for pattern-selective image fusion. *Proc Soc Inform Display.* 1992:467–470.

[24] Burt PJ, Adelson E. The Laplacian pyramid as a compact image code. *IEEE Trans Commun.* 1983;31:532–540.

[25] Olkkonen H, Pesola P. Gaussian pyramid wavelet transform for multiresolution analysis of images. *Graph Models Image Process.* 1996;58:394–398.no.

[26] Rockinger O, Fechner T. Pixel-level image fusion: the case of image sequences. In: *Aerospace/Defense Sensing and Controls*, pp. 378–388. International Society for Optics and Photonics, 1998.

[27] Daubechies I. *Ten Lectures on Wavelets*, vol. 61. Philadelphia: Society for Industrial and Applied Mathematics; 1992.

[28] Mallat SG. A theory for multiresolution signal decomposition: The wavelet representation. *IEEE Trans Pattern Anal Mach Intell.* 1989;11:674–693.no.

[29] Meyer Y. *Wavelets and Operators*, vol. 1. Cambridge University Press; 1995.

[30] Pajares G, Cruz JMDL. A wavelet-based image fusion tutorial. *Pattern Recognit.* 2004;37:1855–1872.no.

[31] Coifman RR, Donoho DL. *Translation-Invariant De-Noising*. New York: Springer; 1995.

[32] Nason GP, Silverman BW. The stationary wavelet transform and some statistical applications. In: *Wavelets and Statistics*. New York: Springer; 1995: 281–299.

[33] Pesquet J-C, Krim H, Carfantan H. Time-invariant orthonormal wavelet representations. *IEEE Trans Signal Process.* 1996;44: 1964–1970.no.

[34] Chai Y, Li HF, Guo MY. Multifocus image fusion scheme based on features of multiscale products and PCNN in lifting stationary wavelet domain. *Opt Commun.* 2011;284:1146–1158.

[35] Rockinger O. Image sequence fusion using a shift-invariant wavelet transform. In: *Image Processing, 1997. Proceedings., International Conference on*, vol. 3, pp. 288–291. IEEE, 1997.

[36] Naidu VPS. Image fusion technique using multi-resolution singular value decomposition. *Defence Sci J.* 2011;61:479.

[37] Liang J, He Y, Liu D, Zeng X. Image fusion using higher order singular value decomposition. *IEEE Trans Image Process.* 2012; 21:2898–2909. no.

[38] Bavirisetti DP, Dhuli R. Two-scale image fusion of visible and infrared images using saliency detection. *Infrared Phys Technol.* 2016;76:52–64.

[39] Bavirisetti DP, Dhuli R. Multi-focus image fusion using multi-scale image decomposition and saliency detection. *Ain Shams Eng J.* 2016.

[40] Zhao J, Feng H, Xu Z, Li Q, Liu T. Detail enhanced multi-source fusion using visual weight map extraction based on multi scale edge preserving decomposition. *Opt Commun.* 2013;287: 45–52.

[41] Jiang Y, Wang M. Image fusion using multiscale edge-preserving decomposition based on weighted least squares filter. *IET Image Process.* 2014;8:183–190.no.

[42] Li S, Kang X, Hu J. Image fusion with guided filtering. *IEEE Trans Image Process.* 2013;22:2864–2875.no.

[43] Bavirisetti DP, Dhuli R. Fusion of infrared and visible sensor images based on anisotropic diffusion and Karhunen-Loeve transform. *IEEE Sensors J.* 2016;16:203–209.

[44] Zhang Z, Blum RS. A categorization of multiscale-decomposition-based image fusion schemes with a performance study for a digital camera application. *Proc IEEE.* 1999;87:1315–1326. no.

[45] Perona P, Malik J. Scale-space and edge detection using anisotropic diffusion. *IEEE Trans Pattern Anal Mach Intell.* 1990;12: 629–639.no.

[46] He K, Sun J, Tang X. Guided image filtering. *IEEE Trans Pattern Anal Mach Intell.* 2013;35:1397–1409. no.

[47] Rosenfeld A, Thurston M. Edge and curve detection for visual scene analysis. *IEEE Trans Comput.* 1971;100:562–569.no.

[48] Petschnigg G, Szeliski R, Agrawala M, Cohen M, Hoppe H, Toyama K. Digital photography with flash and no-flash image pairs. *ACM Trans Graphics.* 2004;23:664–672.no.

[49] Tomasi C, Manduchi R. Bilateral filtering for gray and color images. In: *Computer Vision, 1998. Sixth International Conference on*, pp. 839–846. IEEE, 1998.

[50] Draper NR, Smith H. *Applied Regression Analysis*. John Wiley & Sons; 2014.

[51] Friedman J, Hastie T, Tibshirani R. *The Elements of Statistical Learning*. Berlin: Springer; 2001. Springer Series in Statistics; vol 1.

[52] Durand F, Dorsey J. Fast bilateral filtering for the display of high-dynamic-range images. *ACM Trans Graphics.* 2002;21(3): 257–266.

[53] Shah P, Shabbir NM, Uday BD. An efficient adaptive fusion scheme for multifocus images in wavelet domain using statistical properties of neighborhood. *Information Fusion (FUSION), 2011 Proceedings of the 14th International Conference on*. IEEE, 2011.

[54] Kumar BKS. Image fusion based on pixel significance using cross bilateral filter. *Signal Image Video Process.* 2015;9:1193–1204.

[55] Petrovic V, Xydeas C. Objective image fusion performance characterisation. In: *Tenth IEEE International Conference on Computer Vision (ICCV'05) Volume 1*, vol. 2, pp. 1866–1871. IEEE, 2005.

[56] Qu G, Zhang D, Yan P. Information measure for performance of image fusion. *Electron Lett.* 2002;38:1.

[57] Toet A, Franken EM. Perceptual evaluation of different image fusion schemes. *Displays.* 2003;24:25–37.no.

[58] Xydeas CS, Petrovic V. Objective image fusion performance measure. *Electron Lett.* 2000;36:308–309.no.

How to cite this article: Bavirisetti DP, Kollu V, Gang X, Dhuli R. Fusion of MRI and CT images using guided image filter and image statistics. *Int. J. Imaging Syst. Technol.* 2017;27:227–237. https://doi.org/10.1002/ima.22228